Virology 452-453 (2014) 67–74

Contents lists available at ScienceDirect

Virology

journal homepage: www.elsevier.com/locate/yviro

Construction and characterization of an aureusvirus defective RNA

Pui Kei K. Lee, K. Andrew White *

Department of Biology, York University, 4700 Keele Street, Toronto, Ontario, Canada M3J 1P3

ARTICLE INFO

Article history:
Received 21 November 2013
Returned to author for revisions
8 December 2013
Accepted 23 December 2013
Available online 29 January 2014

Keywords:
Plant virus
RNA virus
RNA recombination
RNA replication
Defective interfering RNA
Aureusvirus
Cucumber leaf spot virus
Tombusvirus
RNA structure
Tombusviridae

ABSTRACT

Defective RNAs (D RNAs) are small RNA replicons derived from viral RNA genomes. No D RNAs have been found associated with members of the plus-strand RNA virus genus *Aureusvirus* (family Tombusviridae). Accordingly, we sought to construct a D RNA for the aureusvirus Cucumber leaf spot virus (CLSV) using the known structure of tombusvirus defective interfering RNAs as a guide. An efficiently accumulating CLSV D RNA was generated that contained four non-contiguous regions of the viral genome and this replicon was used as a tool to studying viral *cis*-acting RNA elements. The results of structural and functional analyses indicated that CLSV contains counterparts for several of the major RNA elements found in tombusviruses. However, although similar, the CLSV D RNA and its components are distinct and provide insights into RNA-based specificity and mechanisms of function.

Introduction

Small RNA replicons derived from plus-strand RNA genomes are useful tools for studying *cis*-acting RNA elements in plant viruses (Simon et al., 2004; Pathak and Nagy, 2009). Some of these replicons are able to accumulate spontaneously when a virus is passaged in plants at high multiplicity of infection (moi) (Li et al., 1989; Burgyan et al., 1991; Rochon, 1991; Rubino et al., 1995). A viral replicon that requires the parental (or helper) genome for reproduction is called a defective RNA (D RNA), while defective interfering RNA (DI RNA) is the term used to describe a replicon that is also able to interfere with virus accumulation and/or host symptoms (White and Morris, 1999).

DI RNAs in plants were first discovered in infections with the plus-strand RNA tombusvirus Tomato bushy stunt virus (TBSV) (Hillman et al., 1987) and these molecules have been studied extensively (White, 1996; White and Nagy, 2004; Nagy, 2008; Pathak and Nagy, 2009; Pathak et al., 2011). A prototypical TBSV DI RNA contains four noncontiguous regions, termed RI through RIV, that are derived from the viral genome. RI corresponds to the 5′-untranslated region (5′UTR), RII encompasses an internal segment, and RIII and RIV are from 3′-proximal and 3′-terminal segments, respectively. The functional RNA elements in each of these regions have been characterized. The active RNA structures in RI include a T-shaped domain (TSD) and a downstream domain (DSD) that are separated by an RNA hairpin (Ray et al., 2003, 2004). The TSD and DSD interact with each other via a pseudoknot termed PK-TD1. In RII, the key structure is an extended stem loop structure, called RII-SL1, and a CC mismatch within RII-SL1 is essential for its function (Monkewich et al., 2005; Pogany et al., 2005). RII also contains a sequence, termed upsteam linker (UL), which interacts with a complementary downstream linker (DL) located in RIII (Wu et al., 2009). The 3′-terminal RIV harbors three RNA stem loop structures and ends with the sequence—CCC$_{-OH}$; the site where minus-strand synthesis initiates (Fabian et al., 2003). This 3′-terminal sequence is complementary to an internal loop of an upstream stem loop structure, termed the replication silencer element (RSE), and this RSE-3′end interaction is important for DI RNA and genome replication (Pogany et al., 2003; Na and White, 2006; Na et al., 2006). Both RII and RIV are essential for TBSV DI RNA accumulation, whereas DI RNAs with either RI or RIII deleted accumulate at low levels (*i.e.*, ~10% that of wild-type) (White and Nagy, 2004).

Members of the genus *Tombusvirus* are most closely related to members of the genus *Aureusvirus*, and both genera are assigned to the family Tombusviridae (Sit and Lommel, 2010). Tombusviruses and aureusviruses are distinct, but they share a common coding organization and corresponding gene functions. The ~4.4 kb long plus-strand RNA genome of the aureusvirus

* Corresponding author. Tel.: +1 416 736 2100x40890/70352; fax: +1 416 736 5698.
E-mail address: kawhite@yorku.ca (K.A. White).

0042-6822/$ - see front matter © 2014 Elsevier Inc. All rights reserved.
http://dx.doi.org/10.1016/j.virol.2013.12.033

Cucumber leaf spot virus (CLSV) is not 5′-capped or polyadenylated and encodes five proteins (Miller et al., 1997) (Fig. 1A, top). Translation of viral proteins is facilitated by a 3′-cap-independent translation enhancer (3′CITE) located in the 3′UTR of the viral genome (Xu and White, 2009). The RdRp, p84, is encoded at the 5′-end of the genome and is expressed via readthrough of the

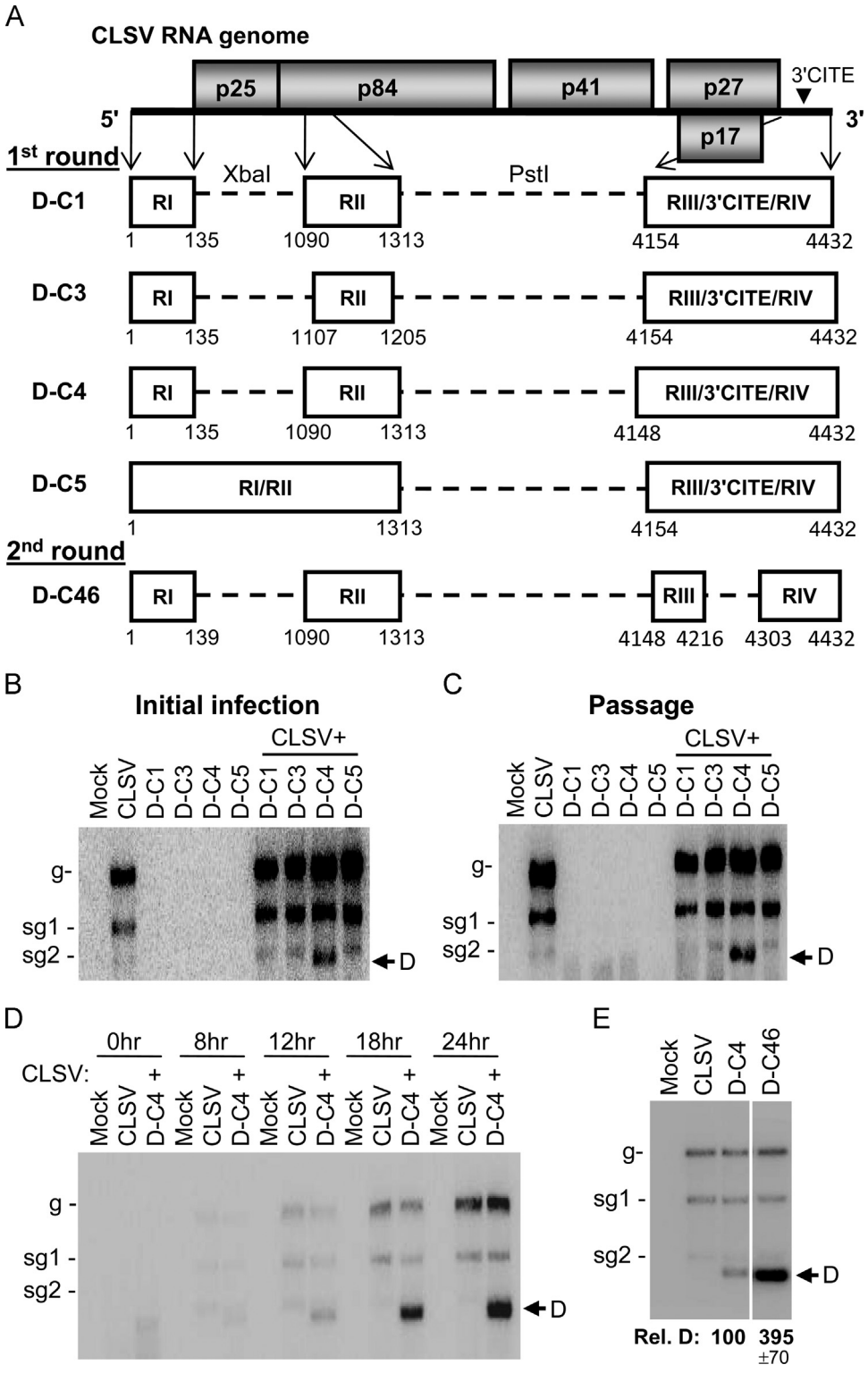

Fig. 1. Accumulation of CLSV genomic and D RNAs. (A) Schematic representation of the CLSV genome and engineered D RNAs. Coding regions of the genome are depicted as shaded boxes that are labeled with respective proteins. The relative position of the 3′CITE in the genome is indicated by the arrowhead. Segments of the genome present in D RNAs are shown below as white boxes (RI, RII, RIII and RIV) with corresponding genomic coordinates. (B) Northern blot of viral RNA accumulation in protoplasts after a 22 h incubation. The viral RNAs used in the transfections are listed above the lanes and the positions of genomic (g), subgenomic (sg) and D RNA (D) are indicated. (C) Aliquots from the infections in panel (B) were used to transfect a second set of protoplasts and the viral RNAs from this passage were analyzed by Northern blotting as described above. (D) Northern blot showing a time course of D RNA accumulation over a 24 h time period. (E) Northern blot of a comparison of D-C4 and D-C46 accumulation levels. Relative D RNA (Rel. D) levels are shown at the bottom, with that for D-C4 set at 100%. In this and other experiments, the means with standard errors are from three independent infections.

5′-proximal open reading frame coding for p25. Both of these proteins are required for genomic RNA replication and subgenomic (sg) mRNA transcription (Reade et al., 2003). The capsid protein (p41) is translated from sg mRNA1 while overlapping silencing suppressor (p27) and movement (p19) proteins are translated from sg mRNA2; both of which are transcribed during infections (Merai et al., 2005; Xu and White, 2008, 2009). Interestingly, although aureusviruses are similar in genomic structure to tombusvirues, no DI RNAs have been found associated with any aureusvirus, even when passaged at high moi (Rubino and Russo, 1997). Accordingly, we sought to construct a DI or D RNA using fragments from the cloned cDNA of the CLSV genome. This endeavor was successful and the resulting functional D RNA was used to characterize *cis*-acting RNA elements in the CLSV genome.

Results

Constructing a D RNA from the CLSV genome

Due to the similarity in genome organization between TBSV and CLSV, the 5′-RI-RII-RIII-RIV-3′ structure of a prototypical TBSV DI RNA was used as a guide to predict corresponding regions in CLSV. First-round CLSV DI RNAs were constructed to contain different portions of the four regions, with restriction enzyme sites introduced at the RI-RII and RII-RIII junctions (Fig. 1A). Potential DI RNAs were screened by coinoculating them with wt CLSV helper genome into protoplasts and examining RNA accumulation following a 22 h incubation. Only one of the candidates, D-C4, accumulated in the initial infection and was still present after passage of this infection (Fig. 1B and C), indicating that it was sustainable and likely replicating. To verify its amplification, D-C4 levels in coinfections were monitored over a 24 h period and were found to increase over time (Fig. 1D). Having identified a replication-competent subviral RNA, two additional modifications were added in an attempt to increase the efficiency of its accumulation. In the second-round candidate, D-C46 (Fig. 1A), four nucleotides were added to RI at its 3′-end so as to include the entire sequence predicted to be involved in a PK-TD1 pseudoknot structure (Fig. 2, green downward bracket). The second modification in D-C46 was removal of an 86 nucleotide long central portion of the 3′CITE located between RIII and RIV (Fig. 1A). In the latter case the deleted sequence was replaced by a GNRA-type tetraloop (Fig. 2, green upward bracket). Both modifications in D-C46 were predicted to lead to enhanced accumulation based on previous analyses of TBSV DI RNAs (White and Morris, 1994; Ray et al., 2003). When tested in helper coinfections, D-C46 accumulated to ~4-fold higher levels than its progenitor D-C4 (Fig. 1E). Interestingly, although D-C46 accumulated efficiently, it did not cause a reduction of the helper genomic or sg mRNAs (Fig. 1E), demonstrating that in protoplasts it functions as a D RNA, not a DI RNA. Accordingly, D-C46 was designated as our model D RNA and used in further structure/function studies.

Structural analysis of a CLSV D RNA

Mfold analysis of CLSV D-C46 revealed the presence of local RNA structures that were similar to those found in each of the four regions in tombusvirus DI RNAs (Fig. 2). The predicted structures were also in good agreement with the results of SHAPE (selective 2′-hydroxyl acylation analyzed by primer extension) solution structure mapping (Fig. 2). The chemical reagent used in this procedure reacts with flexible residues in an RNA structure and the modified sites are detected by primer extension. The more reactive a residue, the more likely it is unpaired in the RNA structure. In the structural model, RI contained a TSD and DSD, separated by a hairpin, and included a potential pseudoknot (PK-TD1). RII formed a Y-shaped structure composed of a lower stem (RII-S3) and two upper stem loops (RII-SL1 and RII-SL2) separated by a UL sequence. A complementary partner for the UL sequence, DL, was identified in RIII. The 3′-portion of RIII was predicted to pair with the 5′-portion of RIV, while the remainder of RIV contained a large stem-loop structure, RIV-SL2, which had an internal loop sequence (i.e., an RSE) that was complementary to a 6 nucleotide long sequence comprising the 3′-terminus of the genome and a portion of a smaller hairpin, RIV-SL1. Overall, the local RNA structures observed in the CLSV D RNA are similar to those present in TBSV DI RNAs.

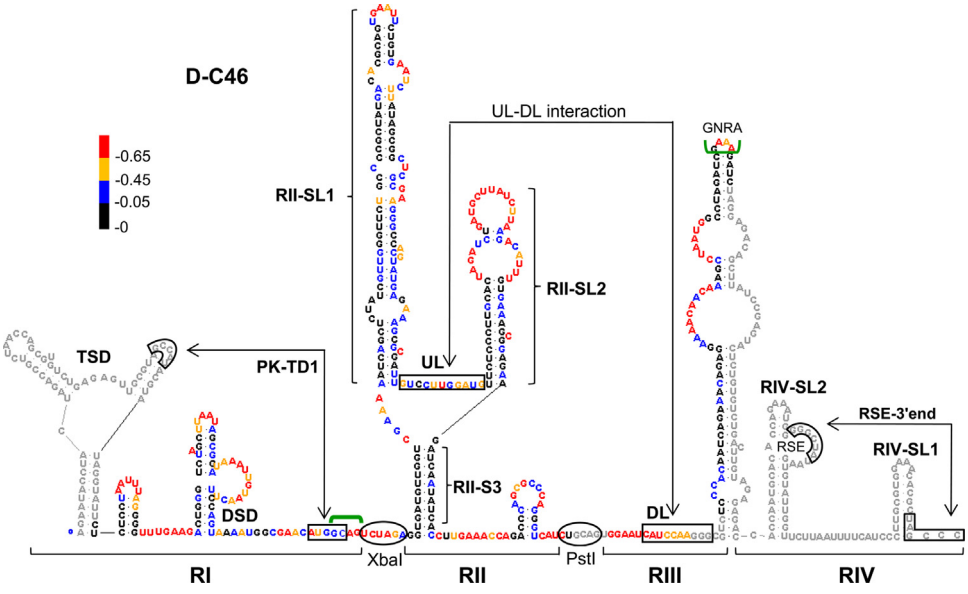

Fig. 2. RNA secondary structure model for D-C46. Mfold-predicted structure for D-C46. The results of SHAPE analysis were mapped onto the mfold-predicted structure. Relative reactivity of each nucleotide is indicated by the color-coded key, with increased flexibility corresponding to higher values. No reactivity data was obtained for the residues depicted in gray. The four regions (RI through RIV) of the D RNA are delineated along with relevant structural domains (*i.e.,* TSD and DSD) and sub-structures (*i.e.,* RII-SL1, RII-SL2, RII-S3, RIV-SL2 and RIV-SL1). Longer-range pairing interactions (PK-TD1, UL–DL and RSE-3′end) are indicated by double-headed arrows and restriction enzyme sites that were introduced are shown within ovals.

Features of RII-SL1 important for D RNA accumulation

The essential nature of RII-SL1 in TBSV replication (Monkewich et al., 2005; Pogany et al., 2005) prompted us to examine its role in CLSV replication using D-C46 as a model replicon. Compensatory mutations designed to disrupt and then restore base pairing were introduced into each of the seven stems in RII-SL1 and the accumulation levels of the resulting mutants were monitored in protoplast coinfections with helper (Fig. 3A, left side). In all cases, destabilizing the stems led to either large decreases or no accumulation of the D RNA. Restoring the stability of the stems revived accumulation for some (S7, S6, S4, S2 and S1) but not all (S5 and S3) mutants. Thus, formation of the majority of the stems in RII-SL1 is important for activity, however S5 and S3 may have additional functional determinants at the level of nucleotide identity.

The demonstrated importance of stem regions in RII-SL1 suggested that they may be involved in the proper presentation of nucleotides in adjacent loop or bulge regions. Accordingly, substitutions or deletions were made in a number of these internal elements to assess their importance (Fig. 3A, right side). Deletion of nucleotides in the two lowest internal loops in mutants L1dC and L2dA inhibited D RNA accumulation, as did deletion of a two nucleotide bulge in L4dGA located further above in RII-SL1. In contrast, deletion of nucleotides in loop 3 either reduced accumulation to ~22% (L3dG) or increased relative levels to ~159% of wild-type (L3dA). L6A, containing an A-to-C substitution near the top of the structure accumulated to near wild-type levels, ~92%. Particular attention was paid to internal loop 5 (C/CUC) as this region corresponded to the critical CC mismatch in RI-SL1 in TBSV (Monkewich et al., 2005; Pogany et al., 2005). Deletion or substitution of the C residue comprising the 5′-half of loop 5 (L5F and L5G) prevented D RNA accumulation. Similarly, substitution of the upper residue (L5A and L5B) or deletion of both lower residues (L5C) in the 3′-half of the loop led to inactivation of the D RNA. However, deletion of one or the other of the latter residues (L5D and L5E) or a substitution of the middle U with A (L5H) yielded viable D RNAs, albeit at different reduced levels. These results indicate that residues in loop 5, as well are those within loops and a bulge in lower regions of RI-SL1, are important for efficient D RNA accumulation.

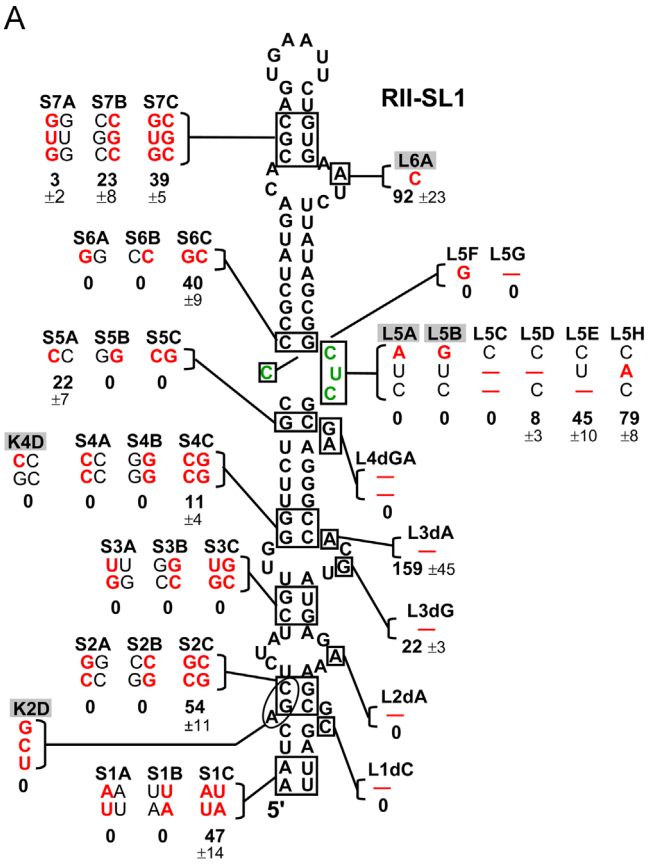

Fig. 3. Mutational analysis of RII-SL1. (A) Mfold-predicted RNA secondary structure for RII-SL1. Residues and base pairs targeted for mutation are shown in boxes. Substitutions are indicated in red and deletions by a red dash. The effects of the mutations on D-C46 accumulation levels were quantified from Northern blot analysis and are presented for each mutant. Shading indicates mutations that were also tested in the context of the CLSV genome. (B) A comparison of relative accumulation levels for D RNA and genomic mutants.

To determine if the effects observed for the D RNA could also be seen in the context of the full-length CLSV genome, several of the mutations were introduced into the wt CLSV infectious clone. Importantly, the mutations selected did not change the identity of the amino acids coding for p84. A total of five mutants were analyzed in protoplast infections, three of which were reported previously, L6A, L5A, and L5B (Nicholson et al., 2012), along with two new mutants, K4D and K2D (Fig. 3A, gray shaded mutants). In all cases, there was good correlation between DI RNA accumulation levels and those of the CLSV genome (Fig. 3B), suggesting that the genome also relies on the same RNA elements for its accumulation.

Both sequence and structure of RIV facilitates D RNA accumulation

Since RIV is a critical component of TBSV DI RNAs, this region was also analyzed in the CIRV D RNA. Interestingly, the predicted structure of the 3′-half of RIV in CIRV contained only two stem loop structures, RIV-SL1 and RIV-SL2 (Fig. 4A), whereas the corresponding region in TBSV contains an additional small hairpin in the intervening segment (Fabian et al., 2003). The CLSV 3′-terminal sequence was complementary to sequence in an internal loop (*i.e.*, the RSE) in RIV-SL2 (Fig. 4A, blue nucleotides). RIV also contained a 9 nucleotide long sequence (Fig. 4A, green nucleotides) that was complementary to a segment in an RNA structure 3′-proximal to the stop codon for p25 (not shown), and this interaction was proposed to facilitate translational readthough leading to p84 synthesis (Cimino et al., 2011). Initially the predicted stem regions in RIV were targeted by compensatory mutational analysis. Disruption and restoration of RIV-SL1 in the T2 series mutants and RIV-SL2 in the T4 and T5 series mutants correlated well with D RNA accumulation levels (Fig. 4A). Substitutions in the UU mismatch in RIV-SL1 in the T1 series mutants revealed that pairing the mismatch was lethal (T1A and T1C), while heterologous pyrimidine mismatches (T1B and T1D) were tolerated, but highly detrimental to accumulation (Fig. 4A). Substitutions in the RSE in RIV-SL2 were completely inhibitory whether (T3A) or not (T9) they were part of the sequence that was complementary to the 3′-terminus. However, the lethal effect of the substitution in T3A was restored to a low level by a compensating change in the 3′-terminal sequence in T3C (Fig. 4**A**). Deletion of one or more residues in the loop outside the region of complementarity either eliminated (T7 and T8) or greatly reduced (T6) D RNA accumulation (Fig. 4A). Finally, the importance of the intervening sequence between the two stem loops was addressed. For this analysis, the 15 nucleotide long tract was divided into three smaller 5 nucleotide long segments.

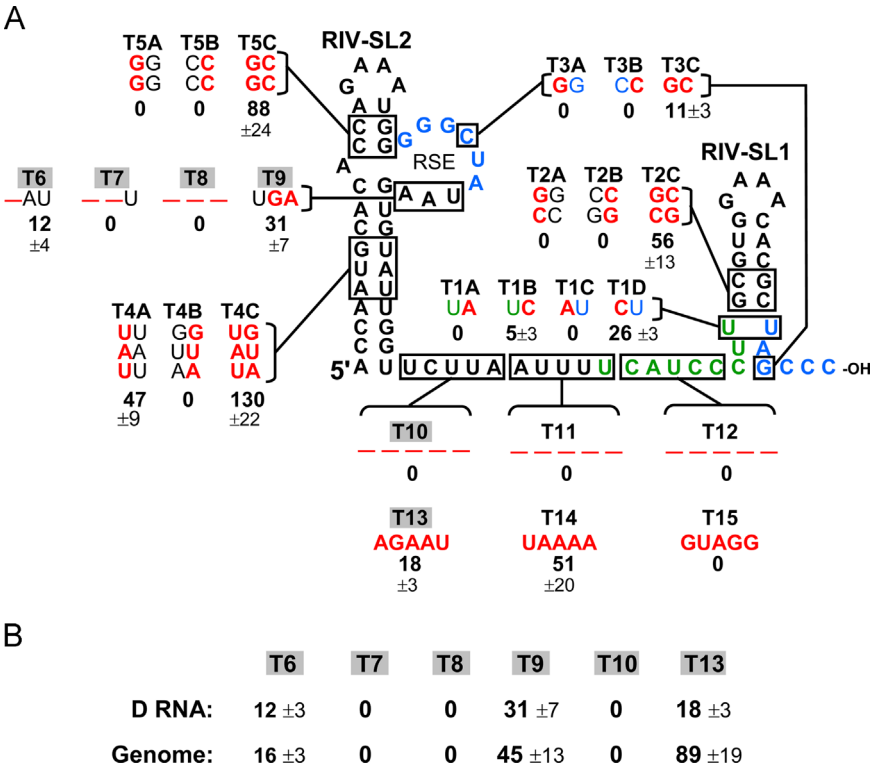

Fig. 4. Mutational analysis of RIV. (A) Mfold-predicted RNA secondary structure for the 3′-portion of RIV. Residues and base pairs targeted for mutation are shown in boxes. Substitutions are indicated in red and deletions by a red dash. Residues involved in the RSE-3′end interaction are in blue and those of the DRTE are in green. The effects of the mutations on D-C46 accumulation levels were quantified from Northern blot analysis and are presented for each mutant. Shading indicates mutations that were also tested in the context of the CLSV genome. (B) A comparison of relative accumulation levels for D RNA and genomic mutants.

Deletion of any of the three segments in T10, T11 or T12 eliminated D RNA accumulation, whereas low, moderate, or no accumulation was observed when the segments were substituted with alternative sequences in T13, T14, and T15, respectively (Fig. 4A). Overall, the results point to important roles for all of the structural components residing in this region.

A number of mutations in RIV were also introduced into the CLSV genome. In general, there was good correlation between the two sets of results (Fig. 4B). The exception being T13, containing a substitution of the first intervening segment, where both replicons were viable but the relative D RNA level (~18%) was ~5-fold less than that of the genome (~89%). This result indicates that certain mutations can be more detrimental to the D RNA than the helper; a consequence that may be due to compensating effects imparted by the more complex genome.

A mid-range interaction in RII mediates D RNA and genome accumulation

The CLSV D RNA also provided an opportunity to investigate longer-range interactions, such as RII-S3 in RII (Fig. 5A). As well, we wanted to assess this mid-range interaction in the context of the full-length genome; however no directly opposing base pairs were present at wobble positions. Consequently, we chose wobble positions located only in the 3′-half of the interaction to introduce substitutions, which were designed to destabilize and then restore stability to RII-S3 (Fig. 5A). In mutant d1, two GC pairs were converted to weaker GU pairs that were predicted to reduce overall stability. This modification reduced relative D RNA levels to ~49% and genome levels to ~87% (Fig. 5B and C). Converting the same two GC pairs to more destabilizing GA mismatches in d2 resulted levels of ~4% and zero for the genome and D RNA, respectively. However, maintaining the GA mismatches and converting an existing central GU to GC in d3 resulted in strong recovery for the genome to ~128% and weaker recovery for the D RNA to ~6%. Notably, strengthening the interaction by converting only the GU to GC in d4 inhibited accumulation of both types of replicons (Fig. 5B and C). These results support an important role for RII-S3 in both D RNA and genome accumulation.

A long-range interaction is required for efficient D RNA and genome accumulation

The potential UL–DL interaction in the D RNA spans a distance of 110 nucleotides, due to the large deletion between RII and RIII (Fig. 2). In contrast, the length of the corresponding intervening sequence in the CLSV genome is 2937 nucleotides (Fig. 6A). To test the importance of the UL–DL interaction in both contexts, a base pair at a wobble position was targeted for compensatory mutational analysis (Fig. 6B). Weakening this base pair led to undetectable levels of both D RNA and genome, while its restoration revived accumulation to ~45% and ~54%, respectively (Fig. 6C and D). Accordingly, both D RNA and genome show a strong dependence on this long-range interaction.

Discussion

Using a prototypical TBSV DI RNA as a guide, we were able to construct the first D RNA for an aureusvirus. Interestingly, unlike TBSV DI RNAs, the CLSV D-C46 was not interfering in protoplast infections, even though it contained similar RNA elements. Compared with typical TBSV DI RNAs, the level of accumulation of D-C46 relative to its helper genome was much less, ~10-fold lower. This lower level of competitiveness could have contributed to reduced interference by limiting sequestration of the viral RdRp

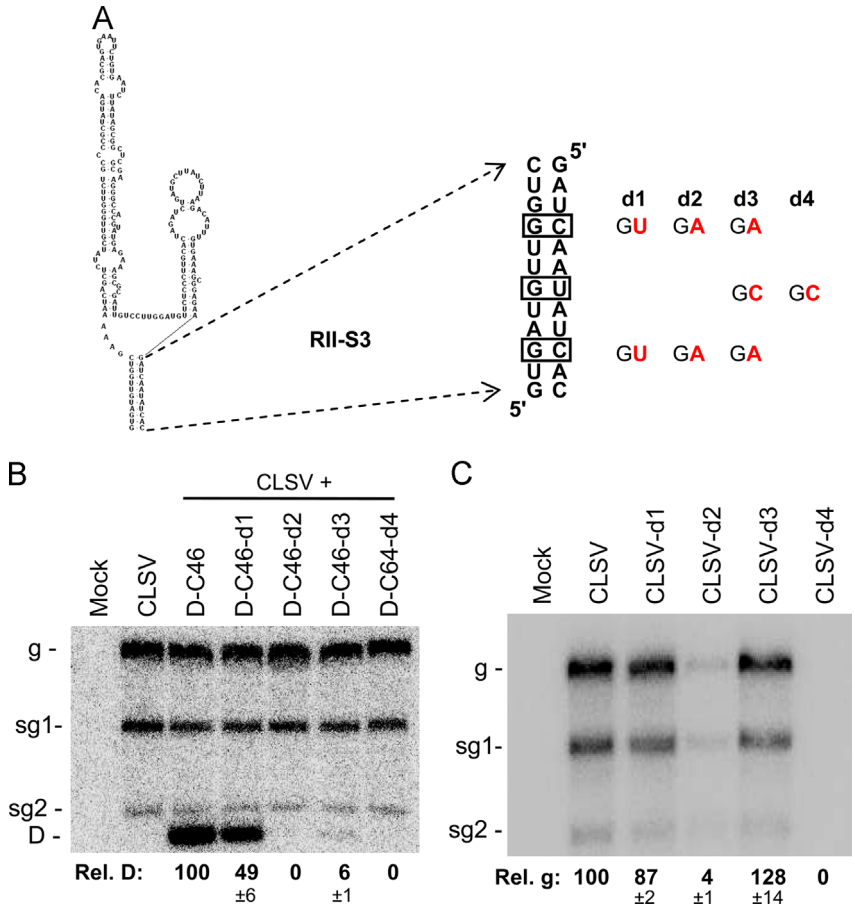

Fig. 5. Mutational analysis of RII-S3. (A) Mfold-predicted RNA secondary structure showing RII-S3. Base pairs targeted for mutation are shown in boxes and substitutions are indicated in red. (B) Northern blot analysis of D RNA mutants depicted in panel (A). (C) Northern blot analysis of the CLSV genomic mutants depicted in panel (A).

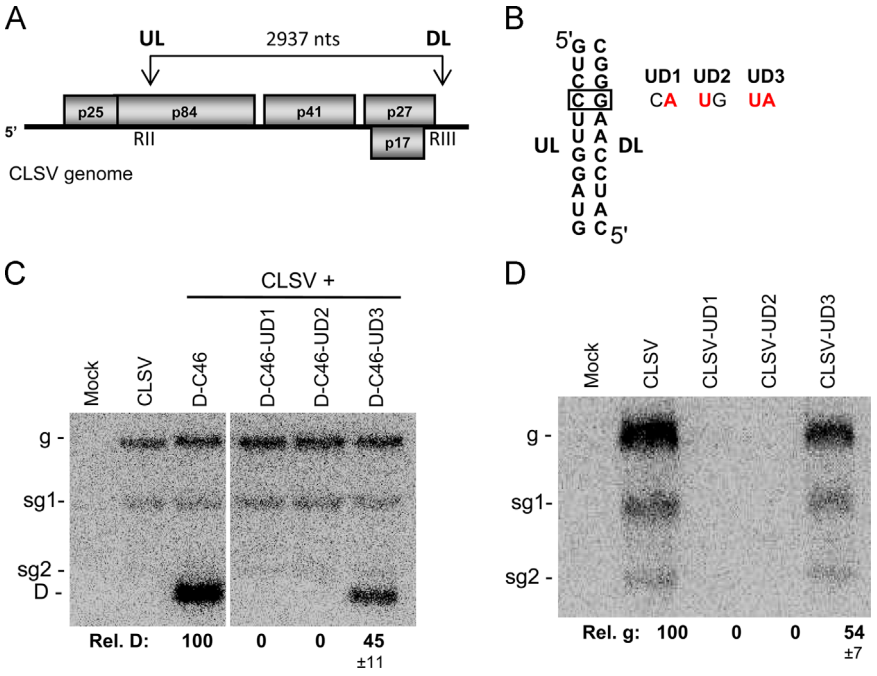

Fig. 6. Mutational analysis of the UL–DL interaction. (A) Schematic representation of the CLSV genome showing the relative locations of the UL and DL sequences. (B) The UL–DL interaction showing the base pair targeted for mutation in a box and substitutions in red. (C) Northern blot analysis of D RNA mutants depicted in panel (B). (D) Northern blot analysis of the CLSV genomic mutants depicted in panel (B).

by the D RNA. Additionally, for tombusvirus DI RNAs, there is evidence that abundant DI RNAs result in high levels of DI RNA-derived siRNAs that saturate the p19 suppressor (Havelda et al., 2005). This in turn causes efficient loading of RISC with the free siRNAs that preferentially target and cleave viral genomic RNA (Havelda et al., 2005; Szittya et al., 2002). Accordingly, another

cause for less interference from D-C46 may have been that its lower level of accumulation was not sufficient to allow for production of a saturating amount of siRNAs. Interfering or not, D-C46 provided a useful new tool for studying *cis*-acting RNA elements involved in CLSV accumulation.

Structural analysis of D-C46 predicted several local RNA structures that were analyzed by mutational analysis. RII-SL1 was determined to be important for D RNA accumulation and mutations in predicted paired and unpaired positions along the length of this extended stem loop structure were inhibitory, indicating that the structural integrity of many subsections contributes to function. One likely role for RII-SL1 is interaction with viral proteins, since the corresponding structure in TBSV is known to bind to the viral replication proteins p33 and p92 (Pogany et al., 2005). In TBSV, a CC mismatch in the central region of its RII-SL1 is a critical determinant of p33/p92 binding, while other regions of the structure are dispensable for binding, but essential for DI RNA accumulation (Pogany et al., 2005; Monkewich et al., 2005). These flanking regions may bind to other protein factors. Similarly, most of RII-SL1 in CLSV appeared to be important for activity and a C/CUC internal loop was located at the same relative position as the CC mismatch in TBSV. Accordingly, the C/CUC may represent an equivalent, but distinct, structural determinant for p25/p84 binding. Indeed, replacement of the C/CUC with the TBSV CC mismatch in mutant L5C led to a nonviable D RNA (Fig. 3). Even replacement of this loop with C/CC in L5D, which is the loop sequence found in two other aureusviruses (Johnsongrass chlorotic stripe mosaic virus and Maize white line mosaic virus), allowed for only 8% accumulation (Fig. 3). The fact that even viruses in the same genera are distinct with respect to this element supports its role as a key determinant of virus specificity.

Other local RNA structures that were examined included two stem loop structures and the intervening sequence in RIV. In comparison with the equivalent terminal region in TBSV, CLSV is unique by lacking an additional small RNA hairpin in its intervening segment. In TBSV, this additional stem-loop, termed SL-2, is essential for replication and a segment of it forms a mutually-exclusive alternative stem-loop structure, SL-T, which is essential for efficient translational readthough of p92 (Cimino et al., 2011). SL-T facilitates readthrough by presenting the distal readthrough element (DRTE) in its terminal loop and the alternating SL-2 and SL-T were proposed to represent an RNA switch that regulates and coordinates minus-strand synthesis and readthrough (Cimino et al., 2011). CLSV contains a putative DRTE (Fig. 4, green), but lacks any associated stem loop structures, therefore if minus-strand synthesis and readthrough are coordinated in CLSV, a mechanism distinct from that used by TBSV must be involved. In this respect, the DRTE in CLSV likely plays a dual function in readthough and viral RNA replication as deletion or substitution of the DRTE in D RNA replicons T12 and T15 abolished their accumulation (Fig. 4).

The stem loops RIV-SL1 and RIV-SL2 were both important for D RNA function. Interestingly, the UU mismatch in RIV-SL1 was also required for maximal activity. Pairing these residues inhibited accumulation (T1A and T1C), while substituted mismatches allowed for low level activity (T1B and T1D) (Fig. 4). The UU mismatch is part of the DRTE (that pairs with its upstream PRTE partner) and the 3′-terminal sequence (that pairs with the RSE in RIV-SL2) (Fig. 4). Consequently, maintenance of the UU mismatch could be related to these alternative pairing functions. Additionally, the mismatch may act to weaken the lower portion of the stem and allow these interactions to occur more efficiently. The residues in the RSE internal loop in RIV-SL2 were also found to be pertinent. A functionally relevant interaction with the 3′-terminal sequence was supported by compensatory mutational analysis (T3 series mutants) (Fig. 4) and this is consistent with similar requirements in both tombusviruses and carmoviruses where the interaction modulates viral RNA replication (Pogany et al., 2003; Zhang et al., 2004). The other residues in the RSE were also determined to be important (mutants T6 through T9) (Fig. 4) and could potentially influence formation of the RSE-3′end interaction.

Longer-range interactions were also found to be important for both D RNA and CLSV genome accumulation (Figs. 5 and 6). A structure equivalent to RII-S3 in RII was recently reported for TBSV (Wu et al., 2013). The precise role of this element remains unclear, but its location near the essential RII-SL1 structure and UL sequence suggested that it could modulate the activity of either of these functional elements (Wu et al., 2013), and the same may be true for CLSV. Interestingly, RII-S3 in CLSV required a certain range of stability, as both increasing (d4) and decreasing (d1 and d2) the wild-type level of stability had negative effects (Fig. 5). This constraint may be related to a required optimal dynamic equilibrium that is perturbed by either strengthening or weakening the interaction. A second much longer-range interaction, the UL–DL interaction, was also required for D RNA and CLSV genome function (Fig. 6). In TBSV, the corresponding interaction acts to relocate the p33/p92 bound to RII to the 3′-terminus and facilitates replicase assembly (Wu et al., 2009). The UL–DL interaction in CLSV likely serves a similar replication-related function, as it was also required in the non-coding D RNA.

The construction of a CLSV D RNA has provided a novel tool to analyze the *cis*-acting RNA elements in aureuviruses and revealed similarities and differences between aureusviruses and tombusviruses. The collective results from both D RNA and genome analyses identified distinct structural determinants of CLSV RNA accumulation and provide a foundation for designing additional studies on aureusvirus replication. It is also worth noting that the CLSV D RNA was not able to accumulate to detectable levels in inoculated or systemically infected leaves in plants coinfected with it and helper (data not shown). This suggests that the failure of prior attempts to detect or generate aureusvirus D or DI RNAs in plants could be related to the inability of such replicons to move efficiently.

Materials and methods

Plasmid construction

The construction of all D RNAs and derivatives of the CLSV genome were carried out using an infectious clone of CLSV (CLSV-JR3; Reade et al., 2003), kindly provided by D′Ann Rochon (Agriculture and Agri-food Canada, Summerland, British Columbia). All mutants were constructed using PCR-based oligonucleotide-mediated mutagenesis and standard recombinant DNA cloning techniques. The PCR-derived regions that were introduced into constructs were sequenced completely to ensure that only the desired modifications were present. The relevant modifications and junction sites in mutant D RNAs and CLSV genomes are presented in the figures of this study.

In vitro transcription and protoplast inoculation

DNA templates used for in vitro transcription were prepared by linearizing the D RNA or CLSV genomic plasmids with SmaI. The AmpliScribe T7-Flash Transcription Kit was used to synthesize viral RNAs according to the manufacturer's instructions. Six to seven day old cucumber cotyledons were used to prepare protoplasts, as previously described (White and Morris, 1994). For each PEG-mediated transfection, $\sim 3 \times 10^5$ protoplasts were inoculated with 3 μg of genomic transcript, with or without 1 μg of D RNA

transcript. Infections were incubated in a growth chamber under fluorescent lighting at 22 °C for 22 h (White and Morris, 1994).

Northern blot analysis

Total nucleic acids were isolated from protoplasts as described previously (White and Morris, 1994). For viral RNA detection, a quarter aliquot of each total nucleic acid preparation was separated in a 1.4% agarose gel and subjected to Northern blot analysis using ^{32}P-5′-end-labeled oligonucleotide probes. All experiments were repeated three times and the means for viral RNA accumulation with standard errors are presented.

RNA secondary structure analysis

RNA secondary structures were predicted at 37 °C using Mfold version 3.6 (Mathews et al., 1999; Zuker, 2003). SHAPE analysis (Mortimer and Weeks, 2007) was performed on in vitro-transcribed D RNA using 1-methyl-7-nitroisatoic anhydride as described previously (Jiwan et al., 2011). Each nucleotide was color coded according to its reactivity score and mapped onto an mMfold-predicted RNA structure. Folding constraints were added to ensure proper formation of core structural elements (*e.g.*, TSD and DSD) and short interactions that were not conserved among aureusviruses were removed to allow for region-based presentation of the core structural elements.

Acknowledgments

We thank D′Ann Rochon for the infectious clone of CLSV and members of our laboratory for reviewing the manuscript. This work was supported by NSERC.

References

Burgyan, J., Rubino, L., Russo, M., 1991. De novo generation of cymbidium ringspot virus defective interfering RNA. J. Gen. Virol. 72, 505–509.
Cimino, P.A., Nicholson, B.L., Wu, B., Xu, W., White, K.A., 2011. Multifaceted regulation of translational readthrough by RNA replication elements in a tombusvirus. PLoS Pathog. 7 (12), e1002423.
Fabian, M.R., Na, H., Ray, D., White, K.A., 2003. 3′-Terminal RNA secondary structures are important for accumulation of tomato bushy stunt virus DI RNAs. Virology 313, 567–580.
Havelda, Z., Hornyik, C., Válóczi, A., Burgyán, J., 2005. Defective interfering RNA hinders the activity of a tombusvirus-encoded posttranscriptional gene silencing suppressor. J. Virol. 79, 450–457.
Hillman, B.I., Carrington, J.C., Morris, T.J., 1987. A defective interfering RNA that contains a mosaic of a plant virus genome. Cell 51, 427–433.
Jiwan, S.D., Wu, B., White, K.A., 2011. Subgenomic mRNA transcription in tobacco necrosis virus. Virology 418, 1–11.
Li, X.H., Heaton, L.A., Morris, T.J., Simon, A.E., 1989. Turnip crinkle virus defective interfering RNAs intensify viral symptoms and are generated de novo. Proc. Natl. Acad. Sci. USA 86, 9173–9177.
Mathews, D.H., Sabina, J., Zuker, M., Turner, D.H., 1999. Expanded sequence dependence of thermodynamic parameters provides robust prediction of RNA secondary structure. J. Mol. Biol. 288, 911–940.
Merai, Z., Kerenyi, Z., Molnar, A., Barta, E., Valoczi, A., Bisztray, G., Havelda, Z., Burgyan, J., Silhavy, D., 2005. Aureusvirus P14 is an efficient RNA silencing suppressor that binds double-stranded RNAs without size specificity. J. Virol. 79, 7217–7226.
Miller, J.S., Damude, H., Robbins, M.A., Reade, R.D., Rochon, D.M., 1997. Genome structure of cucumber leaf spot virus: sequence analysis suggests it belongs to a distinct species within the Tombusviridae. Virus Res. 52, 51–60.
Monkewich, S., Lin, H.X., Fabian, M.R., Xu, W., Na, H., Ray, D., Chernysheva, O.A., Nagy, P.D., White, K.A., 2005. The p92 polymerase coding region contains an internal RNA element required at an early step in Tombusvirus genome replication. J. Virol. 79, 4848–4858.
Mortimer, S.A., Weeks, K.M., 2007. A fast-acting reagent for accurate analysis of RNA secondary and tertiary structure by SHAPE chemistry. J. Am. Chem. Soc. 129, 4144–4145.
Na, H., White, K.A., 2006. Structure and prevalence of replication silencer-3′ terminus RNA interactions in Tombusviridae. Virology 345, 305–316.
Na, H., Fabian, M.R., White, K.A., 2006. Conformational organization of the 3′ untranslated region in the tomato bushy stunt virus genome. RNA 12, 2199–2210.
Nagy, P.D., 2008. Yeast as a model host to explore plant virus-host interactions. Annu. Rev. Phytopathol. 46, 217–242.
Nicholson, B.L., Lee, P.K., White, K.A. 2012. Internal RNA replication elements are prevalent in Tombusviridae. Front Microbiol. 3, 279, http://dx.doi.org/10.3389/fmicb.2012.0.
Pathak, K.B., Nagy, P.D., 2009. Defective interfering RNAs: foes of viruses and friends of virologists. Viruses 1, 895–919.
Pathak, K.B., Pogany, J., Nagy, P.D., 2011. Non-template functions of the viral RNA in plant RNA virus replication. Curr. Opin. Virol. 1, 332–338.
Pogany, J., Fabian, M.R., White, K.A., Nagy, P.D., 2003. A replication silencer element in a plus-strand RNA virus. EMBO J. 22, 5602–5611.
Pogany, J., White, K.A., Nagy, P.D., 2005. Specific binding of tombusvirus replication protein p33 to an internal replication element in the viral RNA is essential for replication. J. Virol. 79, 4859–4869.
Ray, D., Wu, B., White, K.A., 2003. A second functional RNA domain in the 5′UTR of the Tomato bushy stunt virus genome, intra- and interdomain interactions mediate viral RNA replication. RNA 9, 1232–1245.
Ray, D., Na, H., White, K.A., 2004. Structural properties of a multifunctional T-shaped RNA domain that mediate efficient tomato bushy stunt virus RNA replication. J. Virol. 78, 10490–10500.
Reade, R., Miller, J., Robbins, M., Xiang, Y., Rochon, D., 2003. Molecular analysis of the cucumber leaf spot virus genome. Virus Res. 91, 171–179.
Rochon, D.M., 1991. Rapid de novo generation of defective interfering RNA by cucumber necrosis virus mutants that do not express the 20-kDa nonstructural protein. Proc. Natl. Acad. Sci. USA 88, 11153–11157.
Rubino, L., Burgyan, J., Russo, M., 1995. Molecular cloning and complete nucleotide sequence of carnation Italian ringspot tombusvirus genomic and defective interfering RNAs. Arch. Virol. 140, 2027–2039.
Rubino, L., Russo, M., 1997. Molecular analysis of the pothos latent virus genome. J. Gen. Virol. 78, 1219–1226.
Simon, A.E., Roossinck, M.J., Havelda, Z., 2004. Plant virus satellite and defective interfering RNAs: new paradigms for a new century. Annu. Rev. Phytopathol. 42, 415–437.
Sit, T.L., Lommel, S.A., 2010. TombusviridaeEncyclopedia of Life Sciences (ELS)John Wiley & Sons, Ltd, Chichesterhttp://dx.doi.org/10.1002/9780470015902.a0000756.pub2.
Szittya, G., Molnár, A., Silhavy, D., Hornyik, C., Burgyán, J., 2002. Short defective interfering RNAs of tombusviruses are not targeted but trigger post-transcriptional gene silencing against their helper virus. Plant Cell 14, 359–372.
White, K.A., 1996. Formation and evolution of Tombusvirus defective interfering RNAs. Semin. Virol. 7, 409–416.
White, K.A., Morris, T.J., 1994. Nonhomologous RNA recombination in tombusviruses: generation and evolution of defective interfering RNAs by stepwise deletions. J. Virol. 68, 14–24.
White, K.A., Morris, T.J., 1999. Defective and defective interfering RNAs of monopartite plus-strand RNA plant viruses. Curr. Top. Microbiol. Immunol. 239, 1–17.
White, K.A., Nagy, P.D., 2004. Advances in the molecular biology of Tombusviruses, gene expression, genome replication and recombination. Prog. Nucleic Acid Res. Mol. Biol. 78, 187–226.
Wu, B., Grigull, J., Ore, M.O., Morin, S., White, K.A., 2013. Global organization of a positive-strand RNA virus genome. PLoS Pathog. 9 (5), e1003363.
Wu, B., Pogany, J., Na, H., Nicholson, B.L., Nagy, P.D., White, K.A., 2009. A discontinuous RNA platform mediates RNA virus replication: building an integrated model for RNA-based regulation of viral processes. PLoS Pathog. 5 (3), e1000323.
Xu, W., White, K.A., 2008. Subgenomic mRNA transcription in an aureusvirus: down-regulation of transcription and evolution of regulatory RNA elements. Virology 371, 430–438.
Xu, W., White, K.A., 2009. RNA-based regulation of transcription and translation of aureusvirus subgenomic mRNA1. J. Virol. 83, 10096–10105.
Zhang, G., Zhang, J., Simon, A.E., 2004. Repression and derepression of minus-strand synthesis in a plus-strand RNA virus replicon. J. Virol. 78, 7619–7633.
Zuker, M., 2003. Mfold web server for nucleic acid folding and hybridization prediction. Nucleic Acids Res. 31, 3406–3415.